# Reversible Active Site Sulfoxygenation Can Explain the Oxygen Tolerance of a NAD+-Reducing [NiFe] Hydrogenase and Its Unusual Infrared Spectroscopic Properties

Marius Horch,* Lars Lauterbach, Maria Andrea Mroginski, Peter Hildebrandt, Oliver Lenz, and Ingo Zebger*

Institut für Chemie, Technische Universität Berlin, Sekr. PC14, Straße des 17, Juni 135, D-10623 Berlin, Germany

S *Supporting Information*

ABSTRACT: Oxygen-tolerant [NiFe] hydrogenases are metalloenzymes that represent valuable model systems for sustainable H_2 oxidation and production. The soluble NAD^+-reducing [NiFe] hydrogenase (SH) from *Ralstonia eutropha* couples the reversible cleavage of H_2 with the reduction of NAD^+ and displays a unique O_2 tolerance. Here we performed IR spectroscopic investigations on purified SH in various redox states in combination with density functional theory to provide structural insights into the catalytic [NiFe] center. These studies revealed a standard-like coordination of the active site with diatomic CO and cyanide ligands. The long-lasting discrepancy between spectroscopic data obtained *in vitro* and *in vivo* could be solved on the basis of reversible cysteine oxygenation in the fully oxidized state of the [NiFe] site. The data are consistent with a model in which the SH detoxifies O_2 catalytically by means of an NADH-dependent (per)oxidase reaction involving the intermediary formation of stable cysteine sulfenates. The occurrence of two catalytic activities, hydrogen conversion and oxygen reduction, at the same cofactor may inspire the design of novel biomimetic catalysts performing H_2-conversion even in the presence of O_2.
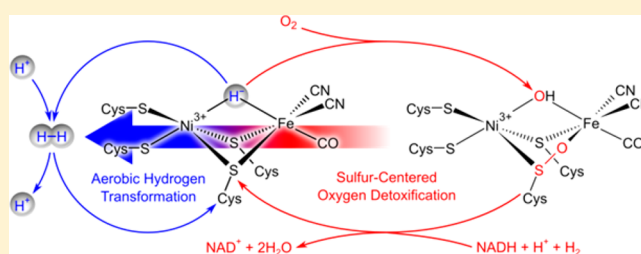
1. INTRODUCTION

In view of anthropogenic global warming and the depletion of carbon-based fossil fuels, future decades will face an inevitable demand for alternative energy sources. Hydrogen has been proposed as an ideally clean fuel storing large amounts of energy, which can be released without producing greenhouse gases.[1] However, a hydrogen-based economy is so far impeded by the lack of sustainable approaches for the production and activation of molecular hydrogen.

Hydrogenases[2] are ancient metalloproteins catalyzing the reversible cleavage of dihydrogen at ambient temperatures. Therefore, they are generally considered as valuable models for sustainable H_2 oxidation and evolution. On the basis of the metal content of the active site,[3,4] these enzymes are classified as [NiFe]-,[5] [FeFe]-,[6] and [Fe] hydrogenases.[7] [NiFe] hydrogenases, which are in the focus of the present study, are versatile catalysts with a bias toward H_2 oxidation.[8] Therefore, they have already been used in biotechnical applications, e.g., as platinum substitutes in biological fuel cells.[9–11] Membrane-bound [NiFe] hydrogenases from sulfur-reducing bacteria have been extensively studied for decades and are generally considered as O_2-sensitive "standard" [NiFe] hydrogenases. These enzymes consist of a large subunit containing the [NiFe] active site and a small subunit carrying an electron relay composed of three FeS clusters (Figure 1A).[5] The binuclear active site contains the two metal ions, Ni and Fe, which are bridged by two cysteinyl thiolates. Two further thiolates serve

as terminal ligands to the Ni, while the Fe ion is additionally coordinated by three diatomic ligands, one CO and two CN^- (Figure 2, top panel).[5,12–14] Different redox states of the active site have been identified by means of infrared (IR) and electron paramagnetic resonance (EPR) spectroscopy.[8] These intermediates differ mainly in the oxidation state of the Ni and the nature of the ligand in the third bridging site between the two metals, while the Fe is generally assumed to remain in the ferrous state throughout the catalytic cycle.

Most [NiFe] hydrogenases are reversibly inhibited by oxygen. Two paramagnetic redox states (Ni^{III}, $S = 1/2$) have been identified for the fully oxidized, oxygen-inhibited active site of standard [NiFe] hydrogenases.[15] While the "ready" Ni_r-B state is easily reduced by incubation with hydrogen within seconds to minutes, reductive reactivation of the "unready" Ni_u-A state may take hours.[16] These observations have been explained by the presence of different oxygen species in the bridging position between the two metals, i.e., a hydroxo species in case of Ni_r-B and, possibly, a (hydro)peroxide in Ni_u-A.[17–19] The molecular structure of the active site in the Ni_u-A state is still under debate;[20] its formation, however, is considered a key-determinant for O_2 sensitivity of standard [NiFe] hydrogenase.
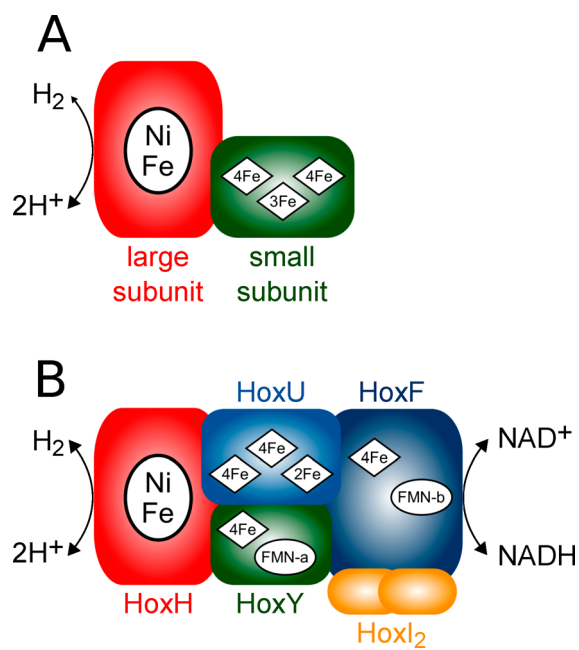
Figure 1. Subunit and cofactor composition of (A) standard [NiFe] hydrogenases and (B) the soluble NAD$^+$-reducing [NiFe] hydrogenase from *Ralstonia eutropha*.[31]
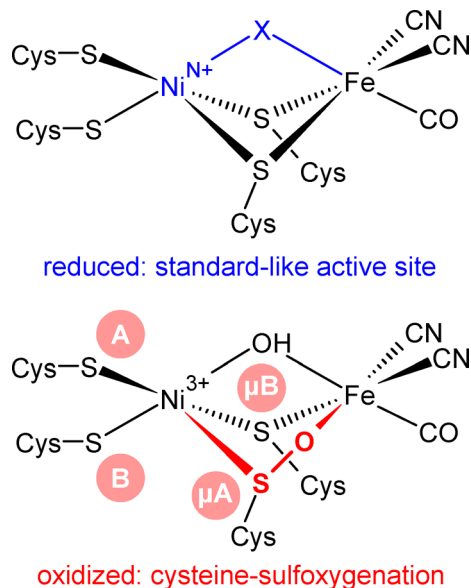

Figure 2. Active site structure of the SH of *R. eutropha*. (Top) A standard-like active site (blue) is verified for the reduced and partly oxidized states, as observed for other [NiFe] hydrogenases.[8,55] (Bottom) For the fully oxidized state (red), the presence of sulfenate species at the active site of the SH is suggested, as shown exemplarily for one of the bridging cysteines. Other possible sulfoxygenation sites are indicated by red circles and labeled according to the respective acronyms. 'X' refers to a vacant coordination site that might be occupied by different ligands. The formal oxidation state of the Ni ion 'N$^+$' assumes values between Ni^I and Ni^{III} in the experimentally observable redox states.[8,55]

Only few [NiFe]-hydrogenases have been shown to catalyze H$_2$ cycling in the presence of ambient O$_2$ levels, and these "oxygen-tolerant" enzymes are of considerable interest for (bio)technologically relevant applications. Consequently, major efforts have been made to elucidate the structural and functional principles underlying O$_2$ tolerance. The four different [NiFe] hydrogenases of the "Knallgas" bacterium *R. eutropha* H16 have been extensively studied as versatile model systems for different biological strategies to cope with high O$_2$ levels.[21]

While the structural basis for oxygen tolerance is so far unknown for the recently characterized actinobacterial hydrogenase,[22] a narrowed gas channel has been proposed to prevent O$_2$ diffusion to the active site in case of the regulatory hydrogenase.[23] In contrast, an unusual [4Fe3S] cluster has been identified in the membrane-bound hydrogenase (MBH) and reported to provide two electrons to the active site, thereby facilitating the reductive detoxification of O$_2$.[24−26] The fourth enzyme is a cytoplasmic NAD$^+$-reducing soluble hydrogenase (SH) that has been studied for more than three decades; yet no crystal structure is available so far. Therefore, the structural and functional determinants for the catalytic activities of this complex biocatalyst, which is O$_2$-tolerant as well,[21,27−31] are still unclear.[31]

The SH is a heteromultimeric metalloenzyme that couples the reversible cleavage of H$_2$ with the interconversion of NAD$^+$ and NADH.[21,27,31] *In vivo*, this enzyme predominantly oxidizes H$_2$, thereby providing reducing equivalents to the cell.[32] In case of an excess of NADH, it acts as an electron valve by reducing protons to H$_2$, which is released by the cells.[33] This oxygen-tolerant enzyme is particularly suited for biotechnological application, e.g., as a cofactor regeneration catalyst and for light-driven H$_2$ production.[34−41]

The SH consists of two different modules (Figure 1B).[21,31] The hydrogenase module is composed of the large subunit HoxH, harboring the [NiFe] active site, and the small subunit HoxY, which presumably contains only one [4Fe4S] cluster and a flavin mononucleotide cofactor (FMN-a).[21,31,42−46] The second module is an NAD$^+$ reductase (diaphorase) unit composed of the HoxF and HoxU subunits. While HoxU harbors two [4Fe4S] clusters and one [2Fe2S] center for electron transfer purposes, the [4Fe4S] cluster-containing HoxF subunit is responsible for the diaphorase activity taking place at the second FMN cofactor (FMN-b).[21,28,31,43,44,46−51] In addition, the SH comprises a homodimeric HoxI$_2$ unit, which presumably has a regulatory role.[52]

Several previous studies have uncovered unusual IR spectroscopic properties for the active site of purified SH. Usually, the diatomic ligands of the active site of [NiFe] hydrogenases give rise to one CO and two CN stretching bands. In contrast, one CO and four CN stretching bands have been observed for the as-isolated SH.[48,50,53,54] This observation led to the misinterpretation that the SH active site is equipped with two additional cyanide ligands, one of which has been related to the O$_2$ tolerance of the enzyme.[48,50,53,54] However, recent *in vivo* EPR and IR spectroscopic experiments have revealed a standard set of diatomic ligands for the catalytic [NiFe] center of the *R. eutropha* SH (Figure 2, top panel),[55] in line with theoretical studies.[31,56] In the course of these experiments, several "standard-like" reduced [NiFe] states have been reported, each represented by one CO and two CN stretching bands. This indicates that H$_2$ cycling of the SH proceeds in a more usual fashion than previously anticipated. Therefore, both the structural basis of the extraordinary O$_2$ tolerance of the SH and a reliable interpretation for the unusual IR spectroscopic signature of the as-isolated enzyme remain to be elucidated. Here, we present IR spectroscopic and theoretical results indicating reversible sulfoxygenation of the

active site cysteines of the SH. This finding is discussed in view of the unusual redox behavior of the SH and its O_2 tolerance.

2. EXPERIMENTAL AND COMPUTATIONAL DETAILS

2.1. Sample Preparation. The SH derived from *R. eutropha* was purified as described previously.[30] For IR spectroscopic investigations, samples were enriched to concentrations between 0.1 and 1 mM. The SH was reduced through incubation with a 50-fold excess of NADH in an anaerobic glovebox for 15 min. For anaerobic reoxidation of reduced SH, NADH was removed from the enzyme solution by buffer exchange using centrifugal filter devices (Amicon Ultra, 30 kDa) in an anaerobic glovebox. Aerobic reoxidation was achieved by the same procedure and an additional incubation with air for 30 min. For *in situ* measurements, *R. eutropha* cells were grown and treated as described previously.[55]

2.2. Infrared Spectroscopy. IR spectra with a spectral resolution of 2 cm^{-1} were recorded on a Bruker Tensor 27 spectrometer, equipped with a liquid nitrogen-cooled mercury cadmium telluride (MCT) detector. The sample compartment was purged with dried air and the sample was held in a temperature-controlled (10 °C) gastight IR-cell for liquid samples (volume ∼7 μL, optical path length = 50 μm), equipped with CaF$_2$ windows. Baseline correction and spectra analysis were performed using the Bruker OPUS software.

2.3. Theoretical Methods. In lack of crystal structure data for the SH, density functional theory (DFT) calculations of vibrational frequencies were performed using a previously established computational model of the isolated [NiFe] hydrogenase active site.[31,56−58] While this type of model tends to systematically under/overestimate the CO/Fe−CO stretching frequencies (see also Supporting Information Section SI 1), relative changes as well as other metal− ligand and intraligand modes of the Fe(CO)(CN)$_2$ moiety are well reproduced.[31,56,58] The obtained results were shown to be comparable to the intrinsic accuracy of DFT and results obtained from quantum mechanical/classical mechanical (QM/MM) hybrid models that explicitly include effects of the protein environment. Furthermore, relative changes in vibrational frequencies, including isotopic shifts, are well reproduced by this computational approach.[58]

Geometry optimizations and frequency calculations were performed on the BP86 level of theory[59,60] in Gaussian 03, using the 6-31g* and tzvp basis sets[61] for H, C, N, O, S atoms and the Ni, Fe atoms, respectively.[56−58,62] Initial geometries for all [NiFe] redox states were derived from the crystal structure of the oxidized *Desulfovibrio gigas* hydrogenase in its Ni$_r$-B state (PDB: 2FRV) by extracting the active site and substituting the −(NH)−C$_α$−(C═O)− peptide moieties with methyl groups (C$_α$H$_3$).[5,56−58] Cartesian coordinates of the C$_α$ atoms of the cysteinates were fixed during structure modification and geometry optimization in order to compensate for the missing protein backbone rigidity, thereby preserving a native-like framework for the active site geometry.[56−58]

For reasons outlined in Supporting Information Section SI 1, we assumed an Fe^{II} Ni^{III}, $S = 1/2$ ground state as well as a Ni$_r$-B-like structure containing a bridging OH$^-$ ligand for structural models of oxidized SH. While other possibilities cannot be excluded, this assumption represents a justified and representative scenario to exemplarily investigate the spectroscopic and functional consequences of the structural variations of interest.

3. RESULTS

To gain insight into the structural basis for the unusual IR spectroscopic properties of purified SH, we first characterized the as-isolated, aerobically oxidized enzyme. As reported previously,[48,50,53,54] the corresponding IR spectrum, henceforth called "split-spectrum", exhibits one intense CO stretching band at about 1957 cm^{-1} and four corresponding CN stretching bands at approximately 2070, 2081, 2090, and 2098 cm^{-1} (Figure 3A). In addition, a weak CO stretching band can be observed at ca. 1972 cm^{-1}, reflecting a structural variant whose CN stretching bands are too weak to be detected
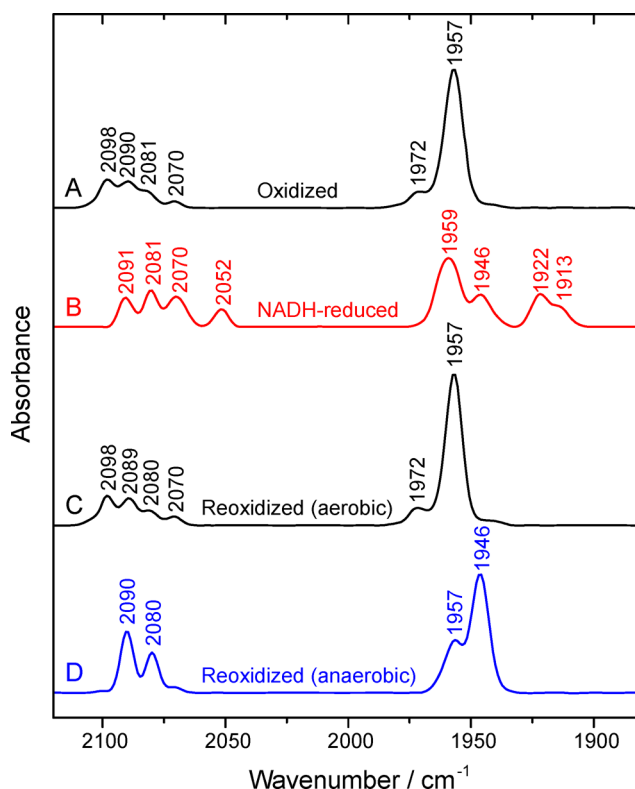

Figure 3. IR spectra of isolated SH showing CO and CN stretching vibrations of the diatomic active site ligands. (A) Oxidized, as-isolated. (B) Reduced with an excess of NADH. (C) Aerobically reoxidized by removal of NADH and subsequent incubation with atmospheric oxygen. (D) Anaerobically reoxidized by removal of NADH. The spectra are normalized with respect to the integral intensity of the range typical for CO stretching vibrations.

in the IR spectrum. These findings are in sharp contrast to results from *in vivo* spectroscopy revealing standard-like redox states, which exhibit each one CO and two related CN stretching bands.[55] Therefore, we recorded the IR spectrum of intact, SH-containing cells (*in vivo*) and compared it to the corresponding spectrum of purified SH isolated from the same cells (*in vitro*). *In vivo*, a complex spectrum reflecting a mixture of standard-like reduced states is observed (Supporting Information Figure SI 1A). Upon purification of the SH, however, this signature is transformed to the typical split-spectrum described above (Supporting Information Figure SI 1B). These observations clearly show that the different IR spectroscopic signatures reported for the SH are not a result of different cell or protein preparations. In contrast, our findings indicate the presence of a conventional [NiFe] site that undergoes structural modifications in response to removal of the SH from its reducing cytoplasmic environment and subsequent exposure to air.

To investigate the reversibility of the structural modifications reflected by the split-spectrum, we incubated as-isolated (oxidized) SH with its natural electron donors, H$_2$ and NADH. While oxidized SH cannot be reduced by H$_2$ alone (data not shown),[50,54,63] previous EPR studies have demonstrated that incubation with an excess of NADH leads to the formation of considerable amounts of the reduced, paramagnetic Ni$_a$-C state (Ni^{III}, $S = 1/2$).[49] Consistently, our IR analysis of NADH-treated SH yielded a complex spectrum reflecting a mixture of several reduced states (Figure 3B, Table

1), which have also been observed *in vivo*.[55] Within this spectrum, individual redox states can be best identified by their

Table 1. Apparent CO and CN Stretching Frequencies Observed for the Different Redox States of *Re* SH[a]

redox species	wavenumber/cm^{-1}	
	$\nu(CO)$	$\nu(CN)$
Ni$_r$-SOX$_{1..n}$	1957	2070
		2080−2081
		2088−2090
		2098
Ni$_r$-B-like	1957 (1957)	2080 (2079)
		2090 (2089)
Ni$_a$-S	1946 (1946)	2080 (2078)
		2090 (2090)
Ni$_a$-C	1959 (1961)	2081 (2080)
		2091 (2091)
Ni$_a$-SR	1946 (1946)	2081 (2080)
		2091 (2090)
Ni$_a$-SR′	1922 (1922)	2052 (2052)
		2070 (2068)
Ni$_a$-SR″	1913 (1913)	2052 (2052)
		2070 (2068)
Ni$_a$-SR2	1959 (1958)	2070 (2068)
		2081 (2080)

[a] 'Ni-SOX$_{1..n}$' refers to a mixture of sulfoxygenated active site species. Values for SH in *R. eutropha* cells are given in parentheses.[55] ν, stretching vibration.

CO stretching bands, which are fairly well separated. Bands at 1946, 1922, and 1913 cm^{-1} indicate contributions from the reduced Ni$_a$-SR, Ni$_a$-SR′, and Ni$_a$-SR″ species, which have also been reported for standard [NiFe] hydrogenases.[8,24] In addition, a broad band at 1959 cm^{-1} can be assigned to a mixture of the Ni$_a$-C (1961 cm^{-1}) and Ni$_a$-SR2 (1958 cm^{-1}) states, the latter of which appears to be a characteristic feature of NAD(H)-converting [NiFe] hydrogenases.[55,64] In conclusion, incubation of as-isolated SH with an excess of NADH demonstrates that structural modifications reflected by the split-spectrum are reversible under conditions that mimic those of the enzyme's cytoplasmic environment.

Removal of NADH from reduced SH and subsequent incubation with atmospheric oxygen results in the typical split-spectrum, demonstrating that the interconversion of reduced species and the oxidized, as-isolated SH is possible in both directions (Figure 3C). Remarkably, this back-conversion was not observed upon mere removal of NADH in the absence of O$_2$. SH treated in this way exhibits an IR spectrum with two CO and essentially two CN stretching bands, indicating a mixture of two standard-like redox states with nearly identical CN stretching frequencies (Figure 3D). The observation of CO and CN stretching bands at 1957 and 2080/2090 cm^{-1} reflects the presence of a Ni$_r$-B-like state, which has been previously observed for oxidized SH in permeabilized cells (*in situ*).[55] The additional CO stretching band at 1946 cm^{-1} was also observed as an intermediate in the course of slow reoxidation of the SH *in situ* (Supporting Information Figure SI 2). This band was found to gain intensity at the expense of the CO stretching band (1961 cm^{-1}) corresponding to the Ni$_a$-C state (Supporting Information Figure SI 2). Consequently, we assign this absorption to the Ni$_a$-S state of the SH, which exhibits CN stretching bands indistinguishable from those of the Ni$_r$-B-like

species. The two different IR spectral signatures observed under aerobic or anaerobic oxidizing conditions strongly indicate that the split-spectrum of as-isolated SH reflects the fully oxidized enzyme, which is formed upon reaction with oxygen.

With the experiments described above, we demonstrated that isolated SH exhibits three types of redox states that can be reversibly interconverted. These are (I) the fully oxidized state, reflected by the split-spectrum, (II) the intermediate oxidized (Ni$_r$-B-like and Ni$_a$-S) states, and (III) several reduced species including the Ni$_a$-C and various Ni$_a$-SR states. While the IR spectra of intermediate oxidized and reduced states exhibit a typical signature of one CO and two CN stretching bands,[31,45,55,56] the fully oxidized, aerobic state is characterized by the characteristic split-spectrum that might be caused by oxidative modifications of the active site.

To elucidate the nature of these possible modifications, we inspected the split spectrum of fully oxidized SH more closely. As stated above, this spectrum exhibits one CO and four instead of two CN stretching bands. Moreover, compared to the CO stretching absorption, the intensity of the four CN bands is considerably lower than usually observed in IR spectra of [NiFe] hydrogenases (approximately 50%). This becomes clear by comparing the split-spectrum in Figure 3C with the spectrum reflecting a mixture of the Ni$_r$-B-like and Ni$_a$-S states in Figure 3D (both normalized with respect to the integral intensity of the CO stretching bands). Likewise, the CN stretching band intensities of fully oxidized SH are also lower by a factor of 2 in comparison to those of the pure Ni$_r$-B-like state, which has been obtained for the as-isolated bidirectional hydrogenase from *Synechocystis* sp. (data not shown).[64] An increased number of CN stretching bands with comparatively low intensities can be *ad hoc* explained by a mixture of two or more states that differ in their CN stretching frequencies while being virtually indistinguishable in terms of the CO stretching vibration. This hypothesis is further supported by variations in the CN stretching pattern, as observed for the split-spectra of different fully oxidized SH preparations (Figure 4). The latter finding is in line with previous reports[50,54] and can be readily explained by varying amounts of individual redox states contributing to that mixture. Consistently, previous studies have also reported IR spectra of individual SH preparations showing only subsets of the four CN stretching bands.[45,50]

We conclude that fully oxidized SH represents a mixture of [NiFe] states, which exhibit structural modifications with a selective impact on the CN stretching modes. This is an unexpected finding since the CO stretching vibration is principally a more sensitive structural marker due to the pronounced σ-donor and π-acceptor capabilities of the CO ligand.[65] As a consequence, selective effects on the CN stretching vibrations suggest structural modifications with a major impact on the equatorial plane of the Fe site, comprising the two CN$^-$ ligands (Figure 2).

In principle, the diatomic ligands of the [NiFe] hydrogenase active site are sensitive toward several structural and electronic factors[65] and, thus, changes in the CO and CN stretching frequencies are often difficult to interpret. However, by observing selective alterations of the CN stretching vibrations, some of the most pronounced effects can be excluded, since these are reflected more readily by alterations of the CO stretching vibration.[65] Therefore, changes in the overall electron density at the active site, e.g., due to variations of the Ni oxidation state, can be ruled out. Furthermore, exchange or removal of the bridging ligand *trans* to the CO molecule
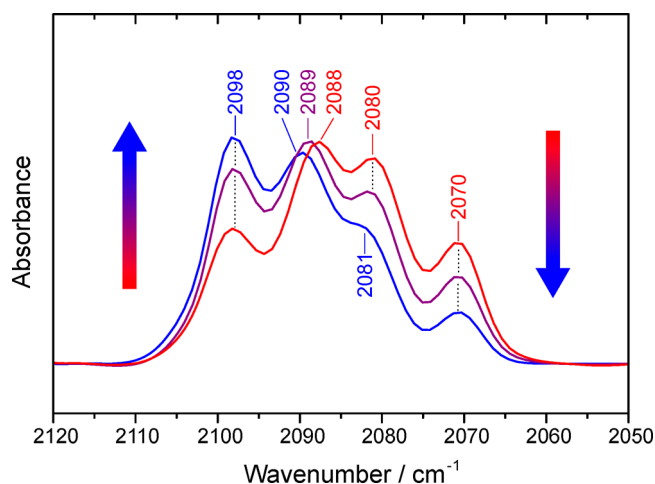
Figure 4. IR spectra of different aerobic preparations of fully oxidized SH displaying the spectral range of CN stretching vibrations. Vertical arrows indicate changes in the observed band intensities. Despite a standardized protocol for the preparation of as-isolated SH,[30] slight variations in cell growth and oxygen exposure during purification cannot be excluded. This may explain differences between the blue and purple spectra. The red spectrum, recorded from an NADH-reduced and subsequently aerobically reoxidized sample, resembles previous preparations of as-isolated SH.[48,71] Spectra are normalized with respect to the integral intensity of the range typical for CO stretching vibrations.

(Figure 2) cannot account for the above observations since this would primarily affect the CO stretching vibration as well. In contrast, alterations of the protein matrix in the vicinity of the CN^- ligands could principally explain the observed spectroscopic effects. In particular, changes in acid−base equilibria of

nearby amino acids might directly or indirectly affect hydrogen bonding of the CN^- ligands to the protein matrix. To examine this possibility, we recorded IR spectra of fully oxidized SH at pH values ranging between 6.2 and 8.0 (Supporting Information Figure SI 3). However, apart from a minor change of the CO stretching frequency, the IR spectra are virtually identical. Thus, alterations of the electrostatics at the active site can hardly account for the splitting of the CN stretching vibrations.

Another possibility to explain selective effects on the CN stretching vibrations are oxidative modifications of the bridging cysteinyl thiolates, which are bound to the same type of Fe orbital as the CN^- ligands (Figure 2, bottom panel). Oxidative modifications are not expected for more reduced redox states, which would explain why the typical split-spectrum is observed for the fully oxidized state, while all other redox states exhibit a standard-like IR spectroscopic signature (Figure 3). Notably, oxidative transformation of terminal and bridging active site cysteinyl thiolates $(R-S^-)$ to the corresponding sulfenates $(R-SO^-)$ has previously been reported for crystal structures of the fully oxidized (Ni_u-A) state of standard [NiFe] hydrogenases.[18−20,66] Likewise, active site cysteine oxygenation was also observed in the crystal structure of a [NiFeSe] hydrogenase.[67] While these modifications may represent irreversible (radiation) damage in some of these enzymes, their observation demonstrates the general possibility to form and stabilize such reactive species at the active site of hydrogenase.

To investigate the impact of possible cysteinyl sulfenates on the IR spectroscopic properties of the $Fe(CO)(CN^-)_2$ moiety, we calculated vibrational frequencies for a large set of sulfoxygenated active site species (Figure 5, Supporting Information Sections SI 5−SI 8). We adopted a previously established computational model of the [NiFe] active site that
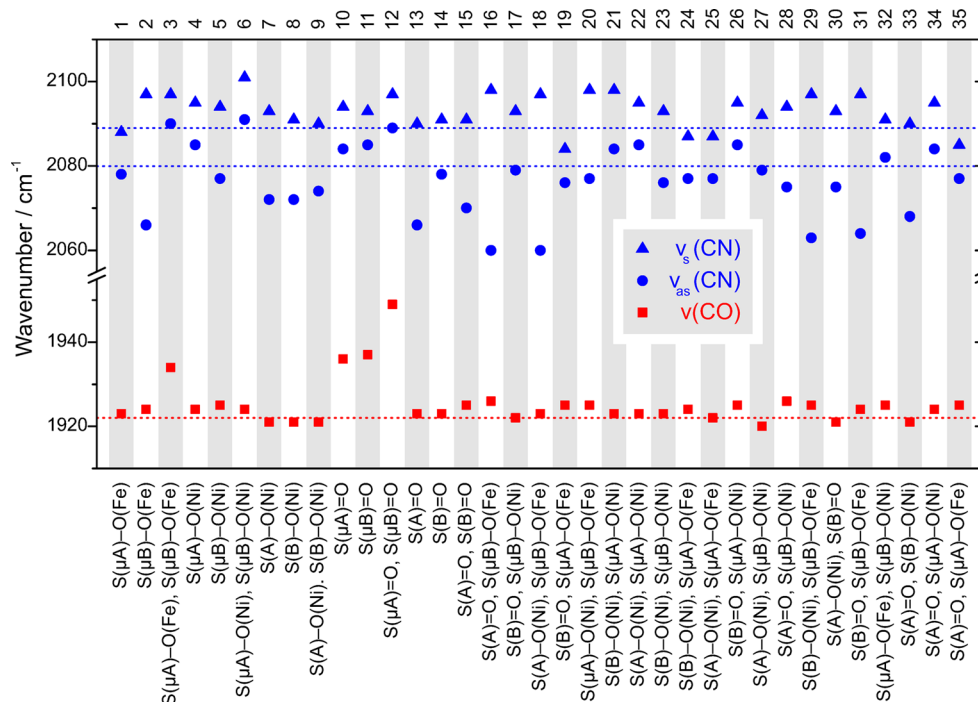

Figure 5. Calculated CO (red) and CN (blue) stretching frequencies for a set of sulfoxygenated active site models. Stretching frequencies of a nonsulfoxygenated reference (Ni_r-B) are shown as horizontal dotted lines. Specific active site sulfenates are denoted in the form S(X)−O(Me), whereby 'X' specifies the site of sulfoxygenation according to Figure 2, and "Me" indicates the metal ion involved in Me−O bonding. S−O and S=O denote species with formal single and double bonds, respectively.

was shown to provide valuable insights into the vibrational properties of the Fe-bound diatomic ligands.[31,56−58] As a basis for the calculations, we assumed a Ni$_r$-B-like structure that is EPR-silent due to antiferromagnetic coupling to another, so far unidentified paramagnetic center,[31,55,68] which is in good agreement with the IR spectroscopic properties (see Supporting Information Section SI 1 for a detailed discussion of this issue). In the following, individual sulfenates will be denoted according to the numbering in Figure 5 and expressed in the form S(X)−O(Me). Here, 'X' specifies the site of sulfoxygenation (see Figure 2, bottom panel) and "Me" indicates the metal ion involved in Me−O bonding. Moreover, notations S−O and S=O denote species with formal single and double bonds, respectively.

As a reference, we first calculated the CO and CN stretching frequencies of the Ni$_r$-B state, which are displayed as horizontal dotted lines in Figure 5. As reported previously for computational models of this type and size,[31,56] the CO stretching frequency of this species is systematically underestimated. However, this fact does not impede the evaluation of relative frequency changes in response to structural modifications (see also Supporting Information Section SI 1).[56,58] Remarkably, the calculated CN stretching frequencies (2080 and 2089 cm^{-1}) are in very good agreement with those of the experimentally observed Ni$_r$-B-like state (2080 and 2090 cm^{-1}),[55] supporting the reliability of the computational approach.

Intriguingly, the presence of one or two sulfenates in bridging or even terminal position has medium to very strong effects on the CN stretching vibrations, while the CO stretching frequency is virtually unaffected in almost all cases (Figure 5). In principle, three different types of CN stretching patterns are observed: (I) In few cases, the modifications have only very small effects on the CN stretching frequencies (e.g., models **1** and **14**), and the calculated IR signatures are almost indistinguishable from the Ni$_r$-B model. (II) Some compounds exhibit a concerted shift of both CN stretching vibrations (e.g., models **6** and **19**), which could explain previous observations of as-isolated SH preparations showing only two CN stretching bands at positions different from those of the Ni$_r$-B-like state.[45,50] (III) In most cases, however, the sulfoxygenations cause an increased frequency separation between the two CN stretching vibrations (e.g., models **16** and **18**).

The calculations demonstrate that the experimentally observed split-spectrum of fully oxidized SH can be easily and consistently explained by a mixture of two or more sulfoxygenated active site species. One suitable scenario would be a mixture of models **1** and **2**, characterized by Fe−O bound sulfenates at either of the two bridging cysteines (Figure 6). Model **1** exhibits a spectrum that is virtually identical to that of the computed Ni$_r$-B state (Figures 5 and 6A), while model **2** reveals an increased splitting of the two CN stretching bands (Figures 5 and 6B). An equimolar mixture of both compounds results in an IR spectrum with one CO and four almost equally spaced, low-intensity CN stretching bands, a pattern that matches the experimental observations (Figures 3A and 6C).

Considering the accuracy of the computational approach, however, additional sulfoxygenated active site species might contribute to the IR split-spectrum as well, in line with the spectral variations observed for different SH preparations (see Figure 4).[50,54] It should be noted that previous X-ray absorption spectroscopy (XAS) studies on the SH suggested an unusual Ni−C/N/O coordination, and this observation was partly related to Ni-bound terminal sulfenates.[63,69−71] Indeed,
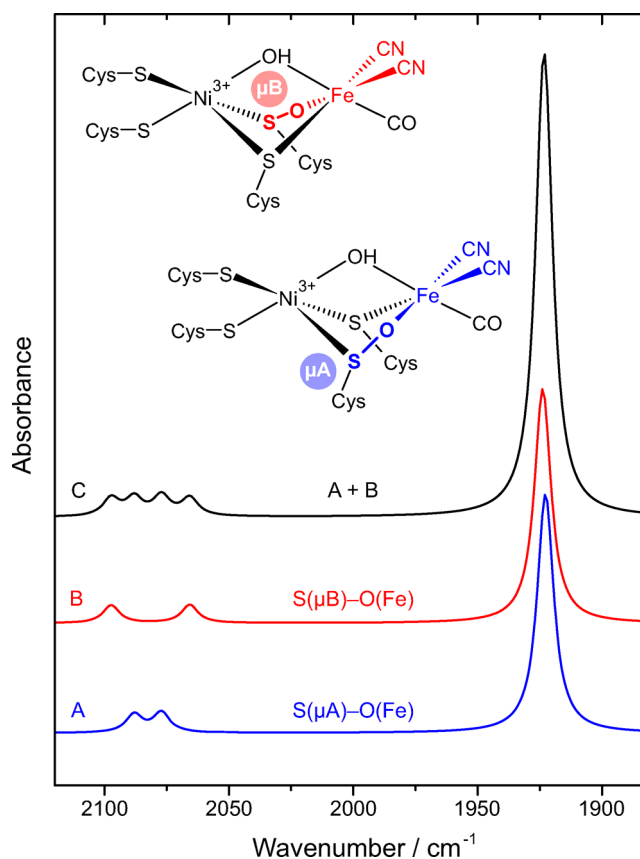

Figure 6. Calculated IR spectra for two active site models exhibiting sulfoxygenation of the bridging cysteines (**1** and **2** of Figure 5), as shown above. (A and B) IR spectra for each of the two models. (C) Sum of spectra A and B, reflecting an equimolar mixture of both species. The IR spectra of both compounds and the corresponding structural depictions are color-coded.

the underlying spectral features were reported to disappear upon reduction of the enzyme with excess NADH or dithionite. This finding is in line with the disappearance of the typical split-spectrum upon reduction of the SH (Figure 3), suggesting that both spectral peculiarities are based on the same oxidation-induced origin. In a previous XAS study, bridging sulfenates were excluded, because such structures would cause alterations in the IR spectrum.[71] This may not be a valid criterion since our calculations show that terminal sulfenates can drastically affect the IR spectrum as well (e.g., models **7** and **13**). Moreover, the SH-typical IR split-spectrum (Figure 3A) represents indeed an unusual IR signature and, consequently, both bridging and terminal Ni−O bound sulfenates might be present in fully oxidized SH preparations. Indeed, calculated frequencies of some of these species resemble the experimental IR spectrum to a reasonable extent. Most notably, an equimolar mixture of models **24** and **29** gives rise to a CN stretching pattern (2063, 2077, 2087, and 2097 cm^{-1}) comparable to that observed experimentally (Figure 3A, Supporting Information Section SI 8). These two compounds are formally identical to the best-fitting models **1** and **2**, except for the additional presence of a terminal sulfenate on the Ni (Figure 5). Notably, models **24** and **29** allow explaining both IR and XAS spectroscopic properties and, thus, such species may contribute significantly to preparations of fully oxidized SH.

There are only few sulfoxygenated models revealing a considerable impact on the CO stretching vibration, i.e., the
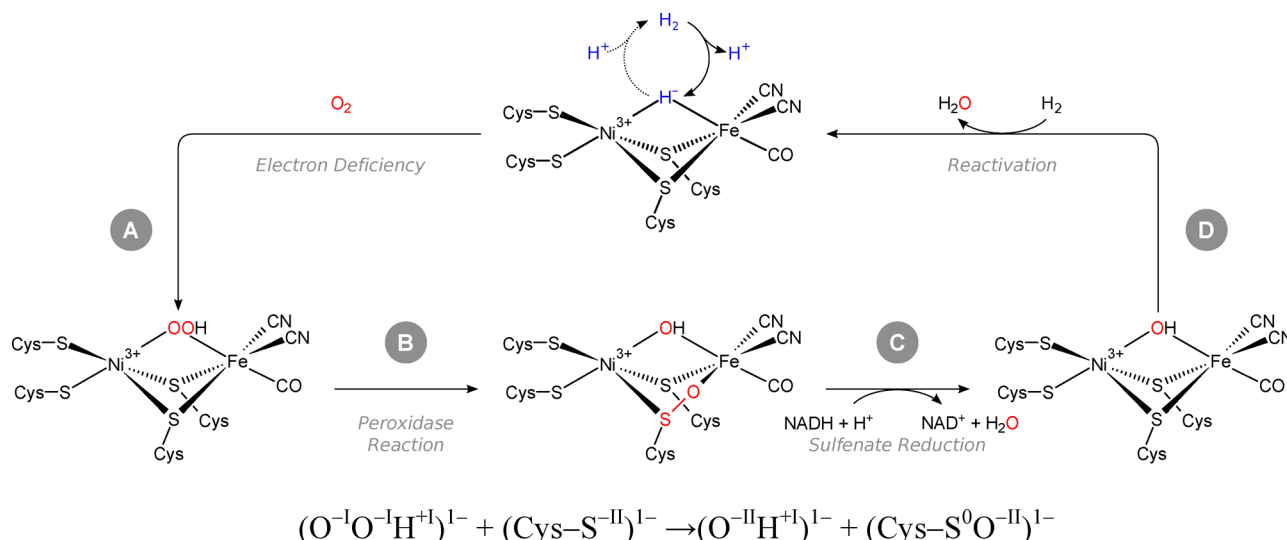
$$(O^{-I}O^{-I}H^{+I})^{1-} + (Cys-S^{-II})^{1-} \rightarrow (O^{-II}H^{+I})^{1-} + (Cys-S^{0}O^{-II})^{1-}$$

Figure 7. Proposed mechanism for the O_2-tolerance of *R. eutropha* SH involving the intermediary formation of sulfenates at the [NiFe] active site. Partial reactions are exemplarily shown for the possible sulfoxygenation of a bridging cysteine (model **1** of Figure 5). Note that essential redox reactions are based on a noninnocent cysteinyl thiolate, while the Ni is not necessarily part of these processes.

frequency is higher compared to the computed Ni_r-B state (e.g., models **11** and **12**). In fact, these modifications may account for minor species of sulfoxygenated SH, manifested in a low-intensity CO stretching band located at higher frequencies (1972 cm^{-1}) in the experimental spectrum (Figure 3A).

In conclusion, all reported IR spectroscopic features of the SH can be explained by the presence of a standard-like active site that exhibits a mixture of reversibly sulfoxygenated species in its fully oxidized state.

4. DISCUSSION

In the present study, we have shown that sulfoxygenation of active site cysteines provides a plausible explanation for the unusual IR split-spectrum observed for fully oxidized SH (Figure 3A). Our results are in line with current and previous experimental data and disentangle the apparent discrepancy between the *in vivo* spectroscopic observation of standard-like reduced states of the active site (Supporting Information Figures SI 1 and SI 2) and former reports on isolated, purified SH.[48,50,53−55] Given the unusual properties of the SH and its remarkable oxygen-tolerance, the observation of oxidative active site modifications in the form of cysteine sulfenates raises the question about their functional significance. In principle, any type of oxygen-derived modification could represent oxidative damage. However, in case of the SH, this is rather unlikely for three reasons. First, the fact that the SH sustains catalytic activity even at high O_2 partial pressure suggests *per se* an insensitivity toward oxidative damage.[21,27−31] Second, the proposed sulfoxygenation of the fully oxidized SH active site appears to be completely reversible upon incubation with an excess of NADH (Figure 3B), which is in line with the high catalytic activities achieved for preactivated enzyme under *in vitro* conditions.[30] Third, the IR split-spectrum of fully oxidized SH (Figure 3A) was previously claimed to correlate with O_2 tolerance, and in fact, this unique spectroscopic signature has only been observed for O_2-tolerant SH protein, but not for its oxygen-sensitive counterparts.[47,48,50,53,54,64] We therefore propose that reversible active site sulfoxygenation plays an important role in the oxygen tolerance of the SH. (Figure 7).

The oxygen sensitivity of standard [NiFe] hydrogenases is generally related to the formation of the fully oxidized, unready Ni_u-A state. Thus, biological strategies of oxygen-tolerance may involve (per)oxidase reactions to prevent or detoxify this species.[8,24−26,30,72] In case of the *R. eutropha* MBH and closely related enzymes, a novel [4Fe3S] cluster has been reported to supply additional electrons to the active site in order to facilitate O_2 detoxification.[8,24−26] The structural basis for O_2 tolerance, however, is presumably different in the SH as no indications for a similar FeS cluster have been observed by Karstens et al.[73] Instead, we propose that oxygen is catalytically detoxified by consecutive two-electron reduction steps involving active site sulfenates as central intermediates (Figure 7).

Under electron-deficient conditions, reaction of the active [NiFe] site with molecular oxygen likely involves the formation of a hydroperoxo species, as previously proposed for the Ni_u-A state (Figure 7A).[74,75] Such a scenario represents a major challenge since hydrogen turnover cannot proceed until the bridging hydroperoxide is removed, and this process has been proposed to be kinetically hindered.[16,19] However, in the presence of cysteine thiolates, a hydroperoxo species can be principally transformed into the corresponding hydroxo counterpart via the formation of a stable sulfenic acid intermediate (Figure 7B).[76] This transformation represents a central step in the proposed oxygen-tolerance mechanism of the SH that requires closer inspection. From a phenomenological point of view, this reaction could be described as a tautomerization in terms of a formal oxygen transfer from the bridging hydroperoxo site toward one of the active site cysteines. In fact, this conversion involves oxidation state changes of both oxygen atoms and the involved sulfur donor. In this respect, the hydroperoxo species contains two oxygen atoms in the oxidation state O^{-I}, while the thiolato sulfur is characterized by an oxidation state of S^{-II}. In contrast, both oxygen atoms are fully reduced to the O^{-II} state in the sulfoxygenated species, while the sulfenato sulfur assumes the increased oxidation state S^0, resulting in the overall redox reaction

$$(O^{-I}O^{-I}H^{+I})^{1-} + (Cys-S^{-II})^{1-}$$
$$\rightarrow (O^{-II}H^{+I})^{1-} + (Cys-S^{0}O^{-II})^{1-}$$
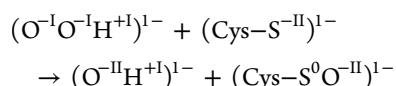
Consequently, this transformation represents a sulfur-based two-electron reduction of a peroxo species as frequently observed in biological systems including those involved in hydrogen peroxide detoxification (non-heme peroxidases).[76−78] In view of the reduction potentials of hydrogen peroxide and sulfenic acids,[76] a high thermodynamic driving force would support this peroxidase reaction, and thus, sulfenate formation via this pathway is expected to be spontaneous and virtually irreversible. As a consequence, the sulfoxygenated product would represent the first stable intermediate upon reaction with oxygen, as observed for fully oxidized SH. This mechanism would ensure that molecular oxygen is already detoxified at an early point of the cycle. However, further reduction steps are necessary to recover catalytically active enzyme. Here, reduction of the sulfenate species represents the most critical step as it requires the reverse flow of two electrons that match the relatively low reduction potential of the sulfenate/thiolate couple (presumably between −100 and −300 mV).[76] Membrane-bound [NiFe] hydrogenases, however, are connected to the high-potential quinone pool (approximately +100 mV) in the cytoplasmic membrane,[3,4,8] and therefore, sulfenate reduction is virtually impossible. For these enzymes, formation of sulfoxygenated species represents a dead end, and consistently, the Ni_u-A state of standard [NiFe] hydrogenases has also been described as a peroxo-derived sulfenate species.[20,66] In contrast, the SH is coupled to the low-potential NADH pool ($E^0 = -320$ mV) in the cytoplasm of the cell.[21,27,31,45,52] Consequently, sulfenates might be readily reduced in a two-electron/two-proton reaction, thereby releasing oxygen in the form of water (Figure 7C). Indeed, catalytic water production as a result of reverse electron flow to the active site has recently been demonstrated for oxygen tolerant [NiFe] hydrogenases including the SH.[30,72] The model is also in agreement with the necessity to reactivate fully oxidized SH with low-potential electrons from, e.g., NADH.[45,48,50,52,54,55,63] The FMN-a molecule proposed to be located close to the catalytic center (Figure 1B) might act as a two-electron transfer unit in analogy to the flavin adenine dinucleotide (FAD) cofactor involved in the sulfur-based detoxification of hydrogen peroxide by NADH peroxidase.[77,78] Indeed, FMN-a has been demonstrated to facilitate both the processes of reductive activation and O_2 reduction in the SH.[30,44,45] Finally, the remaining reaction step of the cycle involves the removal of a bridging hydroxo species (Figure 7D). This process corresponds to the spontaneous (hydrogen-based) activation of the Ni_r-B state in standard [NiFe] hydrogenases,[74,75] which readily proceeds in the SH as well.[55]

In conclusion, using a combined spectroscopic and computational approach, we have shown that the IR spectroscopic properties of the SH can be plausibly explained by a $NiFe(CO)(CN^-)_2$ active site that undergoes cysteine sulfoxygenation in the fully oxidized state. This sulfoxygenation is completely reversible, and thus, it may likely play a key role in the oxygen tolerance of the SH. The underlying mechanism involves the detoxification of an intermediary peroxo species (possibly Ni_u-A) by means of a sulfur-based peroxidase reaction. Electron transfer from active site cysteines could transform the kinetic problem of peroxide removal into a thermodynamic one, i.e., sulfenate reduction. While this process

would likely represent a dead end for standard [NiFe] hydrogenases,[3,4,8,76] it might well represent a feasible reaction for the SH and related enzymes that have access to low-potential electrons from NAD(P)H.[21,27,31,45,52,76−78] Indeed, a similar mechanism has been observed for the flavoprotein NADH peroxidase,[77,78] confirming the biological feasibility of the proposed reaction scheme. The reversible oxygenation of metal-bound sulfur was also observed, e.g., for Ni model compounds, and this observation was discussed in terms of reversible oxidative modifications in [NiFe] hydrogenases as well.[79] Finally, the mechanism suggested for the SH fulfills the central criteria that have been proposed for oxygen tolerance strategies in [NiFe] hydrogenases, namely (per)oxidase activity and the involvement of reverse electron transfer to the active site. However, in contrast to other oxygen-tolerant [NiFe] hydrogenases, the proposed mechanism for oxygen detoxification in the SH is directly centered at the H_2-converting active site. As a consequence, insights into the underlying reactions and intermediates can provide valuable inspiration for the design of bioinspired catalysts that are tolerant toward atmospheric oxygen, thereby providing novel perspectives for hydrogen based energy conversion approaches.

■ ASSOCIATED CONTENT

ⓢ Supporting Information

SI 1, details on structural modeling; SI 2−4, complementary spectroscopic data; SI 5, vibrational frequencies of all computational models; SI 6, structural depictions of all computational models; SI 7, coordinates and energies of all computational models; SI 8, calculated IR spectra for a set of alternative structural models including XAS-predicted terminal Ni−O bound sulfenates This material is available free of charge via the Internet at http://pubs.acs.org.

■ AUTHOR INFORMATION

Corresponding Authors
*marius.horch@gmx.de
*ingo.zebger@tu-berlin.de

Notes
The authors declare no competing financial interest.

■ ACKNOWLEDGMENTS

■ REFERENCES

(1) Hydrogen as a Fuel: Learning from Nature; Cammack, R., Frey, M., Robson, R., Eds; Taylor and Francis: London, 2001.
(2) Stephenson, M.; Stickland, L. H. *Biochem. J.* **1931**, *25*, 205−214.
(3) Vignais, P. M.; Billoud, B.; Meyer, J. *FEMS Microbiol. Rev.* **2001**, *25*, 455−501.
(4) Vignais, P. M.; Billoud, B. *Chem. Rev.* **2007**, *107*, 4206−4272.
(5) Volbeda, A.; Charon, M. H.; Piras, C.; Hatchikian, E. C.; Frey, M.; Fontecilla-Camps, J. C. *Nature* **1995**, *373*, 580−587.
(6) Peters, J. W.; Lanzilotta, W. N.; Lemon, B. J.; Seefeldt, L. C. *Science* **1998**, *282*, 1853−1858.
(7) Shima, S.; Pilak, O.; Vogt, S.; Schick, M.; Stagni, M. S.; Meyer-Klaucke, W.; Warkentin, E.; Thauer, R. K.; Ermler, U. *Science* **2008**, *321*, 572−575.
(8) Shafaat, H. S.; Rüdiger, O.; Ogata, H.; Lubitz, W. *Biochim. Biophys. Acta* **2013**, *1827*, 986−1002.
(9) Karyakin, A. A.; Morozov, S. V.; Karyakina, E. E.; Zorin, N. A.; Perelygin, V. V.; Cosnier, S. *Biochem. Soc. Trans.* **2005**, *33*, 73−75.

(10) Tye, J. W.; Hall, M. B.; Darensbourg, M. Y. *Proc. Natl. Acad. Sci. U.S.A* 2005, *102*, 16911−16912.

(11) Jones, A. K.; Sillery, E.; Albracht, S. P. J.; Armstrong, F. A. *Chem. Commun.* 2002, 866−867.

(12) Volbeda, A.; Garcin, E.; Piras, C.; De Lacey, A. L.; Fernandez, V. M.; Hatchikian, E. C.; Frey, M.; Fontecilla-Camps, J. C. *J. Am. Chem. Soc.* 1996, *118*, 12989−12996.

(13) Happe, R. P.; Roseboom, W.; Pierik, A. J.; Albracht, S. P. J.; Bagley, K. A. *Nature* 1997, *385*, 126.

(14) Pierik, A. J.; Roseboom, W.; Happe, R. P.; Bagley, K. A.; Albracht, S. P. J. *J. Biol. Chem.* 1999, *274*, 3331−3337.

(15) Legall, J.; Ljungdahl, P. O.; Moura, I.; Peck, H. D., Jr.; Xavier, A. V.; Moura, J. J.; Teixera, M.; Huynh, B. H.; DerVartanian, D. V. *Biochem. Biophys. Res. Commun.* 1982, *106*, 610−616.

(16) Fernandez, V. M.; Hatchikian, E. C.; Cammack, R. *Biochim. Biophys. Acta* 1985, *832*, 69−79.

(17) van Gastel, M.; Stein, M.; Brecht, M.; Schröder, O.; Lendzian, F.; Bittl, R.; Ogata, H.; Higuchi, Y.; Lubitz, W. *J. Biol. Inorg. Chem.* 2006, *11*, 41−51.

(18) Ogata, H.; Hirota, S.; Nakahara, A.; Komori, H.; Shibata, N.; Kato, T.; Kano, K.; Higuchi, Y. *Structure* 2005, *13*, 1635−1642.

(19) Volbeda, A.; Martin, L.; Cavazza, C.; Matho, M.; Faber, B. W.; Roseboom, W.; Albracht, S. P. J.; Garcin, E.; Rousset, M.; Fontecilla-Camps, J. C. *J. Biol. Inorg. Chem.* 2005, *10*, 239−249.

(20) Volbeda, A.; Martin, L.; Barbier, E.; Gutiérrez-Sanz, O.; De Lacey, A.; Liebgott, P. P.; Dementin, S.; Rousset, M.; Fontecilla-Camps, J. *J. Biol. Inorg. Chem.* 2015, *20*, 11−22.

(21) Burgdorf, T.; Lenz, O.; Buhrke, T.; van der Linden, E.; Jones, A. K.; Albracht, S. P. J.; Friedrich, B. *J. Mol. Microbiol. Biotechnol.* 2005, *10*, 181−196.

(22) Schäfer, C.; Friedrich, B.; Lenz, O. *Appl. Environ. Microbiol.* 2013, *79*, 5137−5145.

(23) Buhrke, T.; Lenz, O.; Krauss, N.; Friedrich, B. *J. Biol. Chem.* 2005, *280*, 23791−23796.

(24) Saggu, M.; Zebger, I.; Ludwig, M.; Lenz, O.; Friedrich, B.; Hildebrandt, P.; Lendzian, F. *J. Biol. Chem.* 2009, *284*, 16264−16276.

(25) Goris, T.; Wait, A. F.; Saggu, M.; Fritsch, J.; Heidary, N.; Stein, M.; Zebger, I.; Lendzian, F.; Armstrong, F. A.; Friedrich, B.; Lenz, O. *Nat. Chem. Biol.* 2011, *7*, 310−318.

(26) Fritsch, J.; Scheerer, P.; Frielingsdorf, S.; Kroschinsky, S.; Friedrich, B.; Lenz, O.; Spahn, C. M. *Nature* 2011, *479*, 249−252.

(27) Schneider, K.; Schlegel, H. G. *Biochim. Biophys. Acta* 1976, *452*, 66−80.

(28) Schneider, K.; Cammack, R.; Schlegel, H. G.; Hall, D. O. *Biochim. Biophys. Acta* 1979, *578*, 445−461.

(29) Schneider, K.; Schlegel, H. G. *Biochem. J.* 1981, *193*, 99−107.

(30) Lauterbach, L.; Lenz, O. *J. Am. Chem. Soc.* 2013, *135*, 17897−17905.

(31) Horch, M.; Lauterbach, L.; Lenz, O.; Hildebrandt, P.; Zebger, I. *FEBS Lett.* 2012, *586*, 545−556.

(32) Cramm, R. *J. Mol. Microbiol. Biotechnol.* 2009, *16*, 38−52.

(33) Kuhn, M.; Steinbüchel, A.; Schlegel, H. G. *J. Bacteriol.* 1984, *159*, 633−639.

(34) Prince, R. C.; Kheshgi, H. S. *Crit. Rev. Microbiol.* 2005, *31*, 19−31.

(35) Okura, I.; Otsuka, K.; Nakada, N.; Hasumi, F. *Appl. Biochem. Biotechnol.* 1990, *24−25*, 425−430.

(36) Payen, B.; Segui, M.; Monsan, P.; Schneider, K.; Friedrich, C. G.; Schlegel, H. G. *Biotechnol. Lett.* 1983, *5*, 463−468.

(37) Cantet, J.; Bergel, A.; Comtat, M.; Séris, J. L. *J. Mol. Catal.* 1992, *73*, 371−380.

(38) Cantet, J.; Bergel, A.; Comtat, M. *J. Electroanal. Chem.* 1992, *342*, 475−486.

(39) Ratzka, J.; Lauterbach, L.; Lenz, O.; Ansorge-Schumacher, M. B. *Biocatal. Biotransform.* 2011, *29*, 246−252.

(40) Lauterbach, L.; Lenz, O.; Vincent, K. A. *FEBS J.* 2013, *280*, 3058−3068.

(41) Reeve, H. A.; Lauterbach, L.; Ash, P. A.; Lenz, O.; Vincent, K. A. *Chem. Commun.* 2012, *48*, 1589−1591.

(42) Albracht, S. P. J. *Biochim. Biophys. Acta* 1993, *1144*, 221−224.

(43) Schneider, K.; Schlegel, H. G. *Biochem. Biophys. Res. Commun.* 1978, *84*, 564−571.

(44) van der Linden, E.; Faber, B. W.; Bleijlevens, B.; Burgdorf, T.; Bernhard, M.; Friedrich, B.; Albracht, S. P. J. *Eur. J. Biochem.* 2004, *271*, 801−808.

(45) Lauterbach, L.; Liu, J.; Horch, M.; Hummel, P.; Schwarze, A.; Haumann, M.; Vincent, K. A.; Lenz, O.; Zebger, I. *Eur. J. Inorg. Chem.* 2011, *2011*, 1067−1079.

(46) Pilkington, S. J.; Skehel, J. M.; Gennis, R. B.; Walker, J. E. *Biochemistry* 1991, *30*, 2166−2175.

(47) Long, M.; Liu, J.; Chen, Z.; Bleijlevens, B.; Roseboom, W.; Albracht, S. P. J. *J. Biol. Inorg. Chem.* 2007, *12*, 62−78.

(48) Happe, R. P.; Roseboom, W.; Egert, G.; Friedrich, C. G.; Massanz, C.; Friedrich, B.; Albracht, S. P. J. *FEBS Lett.* 2000, *466*, 259−263.

(49) Erkens, A.; Schneider, K.; Müller, A. *J. Biol. Inorg. Chem.* 1996, *1*, 99−110.

(50) van der Linden, E.; Burgdorf, T.; De Lacey, A. L.; Buhrke, T.; Scholte, M.; Fernandez, V. M.; Friedrich, B.; Albracht, S. P. J. *J. Biol. Inorg. Chem.* 2006, *11*, 247−260.

(51) Patel, S. D.; Aebersold, R.; Attardi, G. *Proc. Natl. Acad. Sci. U.S.A.* 1991, *88*, 4225−4229.

(52) Burgdorf, T.; van der Linden, E.; Bernhard, M.; Yin, Q. Y.; Back, J. W.; Hartog, A. F.; Muijsers, A. O.; de Koster, C. G.; Albracht, S. P. J.; Friedrich, B. *J. Bacteriol.* 2005, *187*, 3122−3132.

(53) Bleijlevens, B.; Buhrke, T.; van der Linden, E.; Friedrich, B.; Albracht, S. P. J. *J. Biol. Chem.* 2004, *279*, 46686−46691.

(54) van der Linden, E.; Burgdorf, T.; Bernhard, M.; Bleijlevens, B.; Friedrich, B.; Albracht, S. P. J. *J. Biol. Inorg. Chem.* 2004, *9*, 616−626.

(55) Horch, M.; Lauterbach, L.; Saggu, M.; Hildebrandt, P.; Lendzian, F.; Bittl, R.; Lenz, O.; Zebger, I. *Angew. Chem., Int. Ed.* 2010, *49*, 8026−8029.

(56) Horch, M.; Rippers, Y.; Mroginski, M. A.; Hildebrandt, P.; Zebger, I. *ChemPhysChem* 2013, *14*, 185−191.

(57) Rippers, Y.; Horch, M.; Hildebrandt, P.; Zebger, I.; Mroginski, M. A. *ChemPhysChem* 2012, *13*, 3852−3856.

(58) Horch, M.; Schoknecht, J.; Mroginski, M. A.; Lenz, O.; Hildebrandt, P.; Zebger, I. *J. Am. Chem. Soc.* 2014, *136*, 9870−9873.

(59) Perdew, J. P. *Phys. Rev. B* 1986, *33*, 8822−8824.

(60) Becke, A. D. *Phys. Rev. A* 1988, *38*, 3098−3100.

(61) Weigend, F.; Ahlrichs, R. *Phys. Chem. Chem. Phys.* 2005, *7*, 3297−3305.

(62) Rippers, Y.; Utesch, T.; Hildebrandt, P.; Zebger, I.; Mroginski, M. A. *Phys. Chem. Chem. Phys.* 2011, *13*, 16146−16149.

(63) Burgdorf, T.; Löscher, S.; Liebisch, P.; van der Linden, E.; Galander, M.; Lendzian, F.; Meyer-Klaucke, W.; Albracht, S. P. J.; Friedrich, B.; Dau, H.; Haumann, M. *J. Am. Chem. Soc.* 2005, *127*, 576−592.

(64) Germer, F.; Zebger, I.; Saggu, M.; Lendzian, F.; Schulz, R.; Appel, J. *J. Biol. Chem.* 2009, *284*, 36462−36472.

(65) Darensbourg, M. Y.; Lyon, E. J.; Smee, J. J. *Coord. Chem. Rev.* 2000, *206−207*, 533−561.

(66) Söderhjelm, P.; Ryde, U. *J. Mol. Struct.: THEOCHEM* 2006, *770*, 199−219.

(67) Marques, M. C.; Coelho, R.; De Lacey, A. L.; Pereira, I. A.; Matias, P. M. *J. Mol. Biol.* 2010, *396*, 893−907.

(68) Schneider, K.; Cammack, R.; Schlegel, H. G. *Eur. J. Biochem.* 1984, *142*, 75−84.

(69) Gu, Z.; Dong, J.; Allan, C. B.; Choudhury, S. B.; Franco, R.; Moura, J. J. G.; Moura, I.; LeGall, J.; Przybyla, A. E.; Roseboom, W.; Albracht, S. P. J.; Axley, M. J.; Scott, R. A.; Maroney, M. J. *J. Am. Chem. Soc.* 1996, *118*, 11155−11165.

(70) Müller, A.; Henkel, G.; Erkens, A.; Schneider, K.; Müller, A.; Nolting, H. F.; Sole, V. A. *Angew. Chem., Int. Ed.* 1997, *36*, 1747−1750.

(71) Löscher, S.; Burgdorf, T.; Zebger, I.; Hildebrandt, P.; Dau, H.; Friedrich, B.; Haumann, M. *Biochemistry* 2006, *45*, 11658−11665.

(72) Wulff, P.; Day, C. C.; Sargent, F.; Armstrong, F. A. *Proc. Natl. Acad. Sci. U.S.A.* 2014, *111*, 6606−6611.

(73) Karstens, K.; Wahlefeld, S.; Horch, M.; Gunzel, M.; Lauterbach, L.; Lendzian, F.; Zebger, I.; Lenz, O. *Biochemistry* **2015**, *54*, 389−403.

(74) Armstrong, F. A.; Belsey, N. A.; Cracknell, J. A.; Goldet, G.; Parkin, A.; Reisner, E.; Vincent, K. A.; Wait, A. F. *Chem. Soc. Rev.* **2009**, *38*, 36−51.

(75) Cracknell, J. A.; Wait, A. F.; Lenz, O.; Friedrich, B.; Armstrong, F. A. *Proc. Natl. Acad. Sci. U.S.A.* **2009**, *106*, 20681−20686.

(76) Gupta, V.; Carroll, K. S. *Biochim. Biophys. Acta* **2014**, *1840*, 847−875.

(77) Poole, L. B.; Claiborne, A. *J. Biol. Chem.* **1989**, *264*, 12330−12338.

(78) Yeh, J. I.; Claiborne, A.; Hol, W. G. J. *Biochemistry* **1996**, *35*, 9951−9957.

(79) Darensbourg, M. Y.; Weigand, W. *Eur. J. Inorg. Chem.* **2011**, *2011*, 917−918.